

DETERMINATION OF STELLAR PARAMETERS FOR FGK-DWARF STARS: THE NIR
APPROACH

by

Daniel Thaagaard Andreasen

A thesis submitted in conformity with the requirements
for the degree of Doctor of Philosophy
Graduate Department of Departamento de Física e Astronomia
University of Porto

© Copyright 2017 by Daniel Thaagaard Andreasen

Dedication

To Linnea, Henriette, and Rico

For always supporting me

Acknowledgements

Lorem ipsum dolor sit amet, consectetur adipiscing elit. Ut purus elit, vestibulum ut, placerat ac, adipiscing vitae, felis. Curabitur dictum gravida mauris. Nam arcu libero, nonummy eget, consectetur id, vulputate a, magna. Donec vehicula augue eu neque. Pellentesque habitant morbi tristique senectus et netus et malesuada fames ac turpis egestas. Mauris ut leo. Cras viverra metus rhoncus sem. Nulla et lectus vestibulum urna fringilla ultrices. Phasellus eu tellus sit amet tortor gravida placerat. Integer sapien est, iaculis in, pretium quis, viverra ac, nunc. Praesent eget sem vel leo ultrices bibendum. Aenean faucibus. Morbi dolor nulla, malesuada eu, pulvinar at, mollis ac, nulla. Curabitur auctor semper nulla. Donec varius orci eget risus. Duis nibh mi, congue eu, accumsan eleifend, sagittis quis, diam. Duis eget orci sit amet orci dignissim rutrum.

Nam dui ligula, fringilla a, euismod sodales, sollicitudin vel, wisi. Morbi auctor lorem non justo. Nam lacus libero, pretium at, lobortis vitae, ultricies et, tellus. Donec aliquet, tortor sed accumsan bibendum, erat ligula aliquet magna, vitae ornare odio metus a mi. Morbi ac orci et nisl hendrerit mollis. Suspendisse ut massa. Cras nec ante. Pellentesque a nulla. Cum sociis natoque penatibus et magnis dis parturient montes, nascetur ridiculus mus. Aliquam tincidunt urna. Nulla ullamcorper vestibulum turpis. Pellentesque cursus luctus mauris.

Abstract

Nam dui ligula, fringilla a, euismod sodales, sollicitudin vel, wisi. Morbi auctor lorem non justo. Nam lacus libero, pretium at, lobortis vitae, ultricies et, tellus. Donec aliquet, tortor sed accumsan bibendum, erat ligula aliquet magna, vitae ornare odio metus a mi. Morbi ac orci et nisl hendrerit mollis. Suspendisse ut massa. Cras nec ante. Pellentesque a nulla. Cum sociis natoque penatibus et magnis dis parturient montes, nascetur ridiculus mus. Aliquam tincidunt urna. Nulla ullamcorper vestibulum turpis. Pellentesque cursus luctus mauris.

Resumo

Nam dui ligula, fringilla a, euismod sodales, sollicitudin vel, wisi. Morbi auctor lorem non justo. Nam lacus libero, pretium at, lobortis vitae, ultricies et, tellus. Donec aliquet, tortor sed accumsan bibendum, erat ligula aliquet magna, vitae ornare odio metus a mi. Morbi ac orci et nisl hendrerit mollis. Suspendisse ut massa. Cras nec ante. Pellentesque a nulla. Cum sociis natoque penatibus et magnis dis parturient montes, nascetur ridiculus mus. Aliquam tincidunt urna. Nulla ullamcorper vestibulum turpis. Pellentesque cursus luctus mauris.

Contents

List of Tables	vii
List of Figures	viii
1 Introduction	1
1.1 Exoplanets	2
1.2 Planet host stars	2
1.3 This thesis	2
2 Theory	3
2.1 Stellar structure	3
2.2 Stellar atmosphere	4
2.2.1 Atmosphere models	6
2.2.2 Radiative transfer code -	8
2.2.3 The equivalent width	8
2.2.3.1 Temperature dependence	8
2.2.3.2 Pressure dependence	9
2.2.3.3 Abundance dependence	11
2.2.3.4 Microturbulence	13
2.3 Line list and atomic data	14
2.4 Spectrographs	15
3 Deriving stellar parameters	16
3.1 Photometry	16
3.1.1 InfraRed Flux Method - IRFM	16
3.1.2 T_{eff} -colour-[Fe /H] calibration	17
3.1.3 Asteroseismology	18
3.2 Spectroscopy	19
3.2.1 Synthesis	19
3.3 FASMA	20
3.3.1 Ingredients	20
3.3.2 Wrapper for ARES	21
3.3.3 Interpolation of atmosphere models	22
3.3.4 Minimization	23
3.3.5 Error estimate	26
4 Results for FGK stars	27
4.1 The creation of a NIR line list	27

4.1.1	Measuring the EWs and first filtering	28
4.1.2	Visual removal of lines	29
4.1.3	Synthetic investigation	29
4.1.4	Calibrating the line list: astrophysical $\log gf$ values	31
4.1.5	Removal of high dispersion lines	32
4.2	HD20010	33
4.3	The NIR line list - toward cooler stars	36
4.4	HD 20010 - revisited	39
4.5	Arcturus	39
4.6	10 Leo	40
4.7	Synthetic cool stars	42
4.8	Parameter dependence on EP cut	47
5	SWEET-Cat	48
5.1	What is SWEET-Cat?	48
5.2	Data for 50 planet hosts	49
5.2.1	Proposals for observation time	49
5.2.2	Data collected from proposals	49
5.2.3	Data collected from archive	50
5.3	Analysis of 50 planet hosts	50
5.3.1	Habitable zone	52
5.3.2	Changes to planetary parameters	52
5.3.2.1	HAT-P-46	55
5.3.2.2	HD 120084	55
5.3.2.3	HD 233604	55
5.3.2.4	HD 5583	56
5.3.2.5	HD 81688	56
5.3.2.6	HIP 107773	56
5.3.2.7	WASP-97	57
5.3.2.8	ω Serpentis (ome Ser)	57
5.3.2.9	α Ursa Major (omi UMa)	57
5.4	Discovering two giant planet populations	57
5.5	Future work	58
6	Future work	57
	Bibliography	61

List of Tables

4.1	Summary of the four stars used in this thesis. The stellar parameters are an average from the PASTEL catalogue (Soubiran et al., 2016) (see text for details), except the parameters for the Sun.	27
4.2	Selection of literature values for the atmospheric parameters for HD 20010. The mean and a 3σ standard deviation is presented at the end of the table from the literature values included, which was used as a reference for the derived parameters.	33
4.3	The derived parameters for HD20010 with and without fixed surface gravity.	35
4.4	Results for the three stars where first set of parameters are the literature values as presented in Table 4.1, second set of parameters are results with $\log g$ set to the same value during the minimization procedure as found in the literature (fixed), and last set of parameters are with all parameters free during the minimization procedure.	39
5.1	Columns in SWEET-Cat	49
5.2	Spectrographs used for this paper with their spectral resolution, wavelength coverage, and mean S/N from the spectra used.	50
5.3	Host star and planetary properties of GJ 785, HD 37124, and KELT-6; all which have an exoplanet in the habitable zone.	53
1	Derived parameters for the 50 stars in our sample. The S/N was measured by ARES.	58

List of Figures

2.1	Energy levels for hydrogen, $E_n = \frac{-13.6 \text{ eV}}{n^2}$	7
2.2	An absorption line centred at λ_0 normalised at the flux level F_c . The area of the absorption line to the left is equal to the blue shaded area in the rectangle to the right with width EW.	9
2.3	The EW for a Fe I and Fe II line with increasing T_{eff} . The two lines have similar EW in the Sun and are found in the optical part of the spectrum. The vertical line show the solar T_{eff}	10
2.4	<i>Upper panel:</i> Curve of growth for same Fe II used in Figure 2.3 for four different $\log g$ values. Here it is the weak lines mostly affected by the change in $\log g$. <i>Lower left panel:</i> Synthetic spectra of the same line. The colour scale is the same. <i>Lower right:</i> The abundance for the line at different $\log g$. A strong correlation (0.40) is seen. . .	12
2.5	<i>Upper panel:</i> Curve of growth of the same Fe I line as used in Figure 2.3. Four points are marked which is shown in the <i>lower panel</i> as a synthetic spectral line. The RW (proxy for EW) is clearly increasing with $\log gf$ (proxy for abundance).	13
2.6	Curve of growth for three different values of ξ_{micro} . The EW is increasing with increasing ξ_{micro}	14
3.1	Measured and calculated flux from the Sun at infrared wavelengths. Data from Table 2 in Blackwell and Shallis (1977) . Mean solar radius from this data is $1.011 R_{\odot}$, and mean solar $T_{\text{eff}} = 5963 \text{ K}$ using Equation 3.1.	17
3.2	Mass and radius from asteroseismic scaling relation. The colour is the mass and radius for the upper and lower panel, respectively.	19
3.3	Model atmosphere grid from Kurucz (1993) at $[\text{Fe}/\text{H}] = 0.00$ between 3000 K and 10 000 K. The grid extends to higher T_{eff} , but these are not considered in this thesis.	22
3.4	The abundances of Fe I for the planet host star: HATS-1. Upper plot: Converged parameters (see text for stellar parameters for this star). Middle plot: Converged parameters with 0.5 km/s added to ξ_{micro} . Lower plot: Converged parameters with 500 K added to T_{eff}	24
3.5	Overview of the minimization for FASMA. Credit: Andreasen et al. (2017b)	26
4.1	Solar spectrum (blue) with all iron lines in the spectral region (green) and other elements (orange). The depths and transparencies of the vertical lines are a measure of the line strengths (see Equation 4.1 for details). This is a case where the iron line is discarded due to blending, which is clear in the left wing of the central absorption line.	30

4.2	The three coloured curves represent different iron abundance, $\{-0.20; 0.00; 0.20\}$ compared to solar abundance. The grey curve is the solar atlas for reference. In this case the iron line at $15\,550.439\,\text{\AA}$ was investigated. <i>Upper panel</i> : Synthetic spectra were computed using the full VALD line list in the spectral range for the three different iron abundances. <i>Lower panel</i> : Same as the upper panel, but with the iron line removed from the line list. Since the synthetic spectra shows no features at this absorption line anymore, it is a fair assumption to say the iron line is the cause of this absorption line.	30
4.3	Line abundance of all iron lines before calibrating the $\log gf$ values. The green points are the points with a deviation less than 1.0 dex from the solar iron abundance. All the red points are discarded. The horizontal line shows the solar iron abundance. . . .	31
4.4	The most disperse lines. <i>Upper panel</i> : The MAD versus the original EW. The red points are the outliers which were discarded during this process. <i>Lower plot</i> : Same as above with the de-trended MAD by the exponential fit as shown in the upper panel.	33
4.5	Line identification in piece of Arcturus spectrum with PHOENIX model and telluric model for correcting RV.	35
4.6	Difference in abundance for HD 20010 when multiple measurements of EW were obtained. The differences are between the lowest and highest measured EW in case of multiple measurements. This is shown against the wavelength (<i>upper panel</i>) and in a histogram (<i>lower panel</i>).	36
4.7	Comparison of the EW from the first version of the line list, EW_1 , and the second version, EW_2 . The EWs are generally higher in the second version, with an average difference between the two version of $(2.1 \pm 11.1)\,\text{m\AA}$. The three horizontal lines show the average value and the standard deviation.	38
4.8	Top figure: Difference of the automatic EW measurements between the summer observations and winter observations from the Arcturus spectra. Bottom figure: Same as above, but with manual measurements from ARES (summer) and automatic measurements (summer).	41
4.9	Derived parameters of 12 synthetic PHOENIX spectra with varying T_{eff}	43
4.10	Derived parameters of 12 synthetic PHOENIX spectra with varying T_{eff} . Here $\log g$ is fixed at 4.5 dex and ξ_{micro} fixed according to an empirical relation, thus only deriving T_{eff} and $[\text{Fe}/\text{H}]$	44
4.11	Common EWs between Arcturus and the synthetic spectrum with closest parameters (see text for details). The EWs are getting more disperse with increasing EW which is expected when seeing the direct comparison of the spectrum in Figure 4.12.	45
4.12	Comparison between the Arcturus atlas and a PHOENIX synthetic spectrum with similar parameters to Arcturus (see text for details).	45
4.13	Derived $[\text{Fe}/\text{H}]$ with respect to the true T_{eff} for runs that reached convergence. <i>Top panel</i> : $\log g$ fixed at 4.5 dex and ξ_{micro} to the empirical relation (see text for details). <i>Lower panel</i> : All parameters free.	46
5.1	A Hertzsprung-Russell diagram of the sample of 50 planet host stars added to SWEET-Cat. The parameters were derived using optical high resolution and high S/N spectra in tandem with FASMA and an optical line list. The colour scale shows the derived $\log g$ for each star.	51

5.2	The habitable zone for the updated SWEET-Cat stars. The coloured line shows the theoretical habitable zone, while the dots shows the location of the planets in the actual system. The blue lines show the habitable zone of the three stars where a planet is located within it (green points). The red dots and orange lines are systems which does not lie within the habitable zone.	53
5.3	Stellar radius on both axes calculated based on Torres et al. (2010) . The x-axis shows the stellar radius based on the atmospheric parameters from the literature, while the y-axis indicates the new homogeneous parameters presented here. The colour and size indicate the surface gravity. This clearly shows that the disagreement is biggest for more evolved stars.	54
5.4	Giant planet masses for the full sample and constrained sample (see text for details). This study was performed by Santos et al. (2017) to distinct two giant planet populations.	58

Chapter 5

SWEET-Cat

Part of the work during the thesis has been dedicated to regularly update SWEET-Cat¹, a catalogue with all discovered planet hosts, and the stellar parameters.

In this chapter a detailed description of SWEET-Cat will be presented. Moreover an analysis of 50 planet hosts was performed during the thesis with updated planetary parameters (mass and radius).

5.1 What is SWEET-Cat?

As mentioned above, SWEET-Cat is a catalogue of planet host stars. However, the strength of SWEET-Cat is the homogeneously analysed stars utilising the method described in Section 3.3 with FASMA or a similar tool before the creation of FASMA.

In the era with a large number of discovered exoplanets (more than 3500 confirmed exoplanet at the moment of writing), the time for in-depth statistical studies has arrived. However, when conducting these studies it is crucial to have consistent measurements of e.g. stellar atmospheric parameters. This can be obtained by using a single analysis to obtain these parameters, as it is known that different methods will lead to different results (see e.g. [Hinkel et al., 2016](#), for a recent review).

To obtain stellar atmospheric parameters from one method is an on-going goal with SWEET-Cat, where high quality spectra are obtained for stars hosting planets. These are used to determine the stellar parameters in a homogeneous way. All stars in SWEET-Cat analysed with the method from our group are marked with a flag showing whether it is analysed homogeneously or not. The columns provided in SWEET-Cat are summarised in Table 5.1. It is important to note that SWEET-Cat does not include any planetary parameters.

SWEET-Cat is updated on a weekly basis if new planet hosts are discovered, and whenever planet hosts have been analysed with the method from our group, as described in this thesis.

¹ <https://www.astro.up.pt/resources/sweet-cat/>

Table 5.1: Columns in SWEET-Cat

Column	Unit	Description
Name		Popular stellar name
HD number		HD number
RA	deg	Right ascension
Dec	deg	Declination
Vmag	mag	V magnitude
$\sigma(\text{Vmag})$	mag	Error on V magnitude
π	mas	Parallax
$\sigma(\pi)$	mas	Error on parallax
Source of π		Source of parallax measurement
T_{eff}	K	Effective temperature
$\sigma(T_{\text{eff}})$	K	Error on effective temperature
$\log g$	dex	Surface gravity
$\sigma(\log g)$	dex	Error on surface gravity
$\log g_{\text{LC}}$	dex	Surface gravity corrected from light curves
$\sigma(\log g_{\text{LC}})$	dex	Error on surface gravity corrected from light curves
ξ_{micro}	km/s	Micro turbulence
$\sigma(\xi_{\text{micro}})$	km/s	Error on micro turbulence
[Fe / H]	dex	Metallicity
$\sigma([\text{Fe} / \text{H}])$	dex	Error on metallicity
Mass	M_{\odot}	Stellar mass
$\sigma(\text{Mass})$	M_{\odot}	Error on stellar mass
Reference		Reference for parameters
Homogeneity flag	0/1	0 for not homogeneous analysis, 1 otherwise
Last updated	date	Last updated
Comments		Any special remarks/comments (e.g. M star)

5.2 Data for 50 planet hosts

In this section the data for a large update to SWEET-Cat will be described. The majority of the data comes as a result from proposals submitted for observational time, while some of the data was found in the archive. In the next section the analysis of the 50 spectra will be presented along with the results.

5.2.1 Proposals for observation time

5.2.2 Data collected from proposals

Data for 43 out of the 50 stars were collected by the SWEET-Cat team using the UVES/VLT (Dekker et al., 2000), FEROS/2.2m telescope in La Silla (Kaufer et al., 1999), and FIES/NOT (Frandsen and Lindberg, 1999) spectrographs. The remaining spectra were found in various archives. This includes spectra from the HARPS/3.6m telescope in La Silla (Mayor et al., 2003) and ESPaDOnS/CFHT (Donati, 2003). Some characteristics of the spectrographs are presented in Table 5.2 with the mean

S/N for the spectra used. The S/N for each star can be seen in Table 4.4 along with the atmospheric parameters of the stars. The S/N is measured automatically by ARES, but we note that ARES smooths the spectra before measuring the S/N, hence it is listed higher than the actual S/N. These 50 stars are confirmed exoplanet hosts listed in SWEET-Cat. However, they belonged to the list of stars that have not been analysed by our team. We therefore increase the number of stars analysed in a homogeneous way, which is the goal of SWEET-Cat.

We obtain the spectra with the highest possible resolution for a given spectrograph, and in cases with multiple observations, we include all the observations unless a spectrum is close to the saturation limit for a given spectrograph. For multiple spectra, we combine them after first correcting the radial velocity (RV) and using a sigma clipper to remove cosmic rays. The individual spectra are then combined to a single spectrum for a given star to increase the S/N. This single spectrum is used in the analysis described below. For most of the spectra in the archive included here, several spectra were combined as described above, while for the observations dedicated to this work, the spectrum would be a single spectrum, or in cases of faint stars, it would be observed a few times to reach the desired S/N. This is mostly due to the difference in science cases behind the observations; for example, the HARPS spectra were used for RV monitoring or follow-up of the exoplanet(s), while the UVES spectra were used to characterise stellar parameters.

Table 5.2: Spectrographs used for this paper with their spectral resolution, wavelength coverage, and mean S/N from the spectra used.

Spectrograph	Resolution	Spectral range	Mean S/N
HARPS	115 000	378 nm to 691 nm	642
UVES	110 000	480 nm to 1100 nm	212
ESPaDOnS	81 000	370 nm to 1050 nm	775
FIES	67 000	370 nm to 730 nm	763
FEROS	48 000	350 nm to 920 nm	208

5.2.3 Data collected from archive

5.3 Analysis of 50 planet hosts

The method of determining atmospheric parameters from the curve of growth analysis has been applied several times in the optical (see e.g. [Mortier et al., 2013b](#); [Santos et al., 2013](#); [Sousa et al., 2011](#); [Tsantaki et al., 2013](#)). When studying stars with planets and any correlations between stellar and planetary parameters it is important to have a homogeneous characterisation of the stars. An effort to create such a sample was initiated by [Santos et al. \(2013\)](#) with the SWEET-Cat database. The motivation to homogenise the stellar hosts is mainly to compare the hosts and make statistical studies on one consistent scale. When doing these statistical studies, the results might otherwise suffer from offsets between different methods.

The skills acquired during the NIR studies as mentioned above were directly translated into deriving parameters for a sample of 50 known planet host stars that were not previously analysed by our group ([Andreassen et al., 2017b](#)). The spectra of these stars were required at UVES, FIES, HARPS, and ESPaDOnS with the mean S/N higher than 200.

A Hertzsprung-Russell diagram of the sample can be seen in Figure 5.1. The sample covers a large range of T_{eff} , FGK, while there are both dwarf, sub-giant, and some giant stars. The colours indicate the $\log g$. In order to determine the luminosity of each star the simple relation

$$L = 4\pi R^2 \sigma T_{\text{eff}}^4$$

is used, where L is the luminosity, R is the stellar radius, and σ is the Stefan-Boltzmann constant. In solar units this relation is simply:

$$\frac{L}{L_{\odot}} = \left(\frac{R}{R_{\odot}} \right)^2 \left(\frac{T_{\text{eff}}}{T_{\text{eff},\odot}} \right)^4$$

In order to determine the the stellar radius, the empirical relation from [Torres et al. \(2010\)](#) was used.

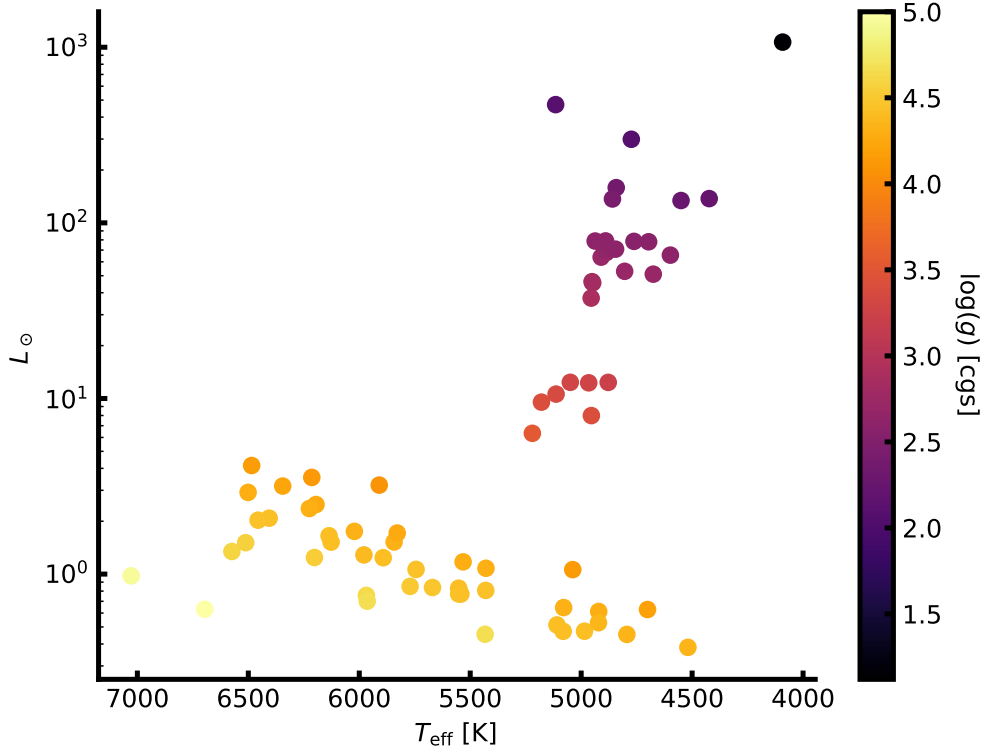


Figure 5.1: A Hertzsprung-Russell diagram of the sample of 50 planet host stars added to SWEET-Cat. The parameters were derived using optical high resolution and high S/N spectra in tandem with FASMA and an optical line list. The colour scale shows the derived $\log g$ for each star.

The parameters were derived using FASMA with the optical line list compiled by [Sousa et al. \(2008\)](#) and [Tsantaki et al. \(2013\)](#) for stars where T_{eff} was below 5200 K. All the new derived parameters were added to SWEET-Cat, available for the community.

A correction to the spectroscopic surface gravity ($\log g_{\text{spec}}$) is applied based on asteroseismology as found by [Mortier et al. \(2014\)](#) given by:

$$\log g_{\text{seis}} = \log g_{\text{spec}} - (3.89 \pm 0.23) \times 10^{-4} T_{\text{eff}} + 2.10 \pm 0.14, \quad (5.1)$$

where $\log g_{\text{seis}}$ is the corrected surface gravity. This correction is only used for FGK dwarf stars, i.e. between $4800 \text{ K} \leq T_{\text{eff}} \leq 6500 \text{ K}$ and $\log g \geq 4.2 \text{ dex}$. For stars with a $\log g$ lower than this limit the correction will not be applied, and if the $\log g$ changes to below this limit after the correction, the spectroscopic $\log g$ will be used again. The correction for $\log g$ depends on both T_{eff} and $\log g$. The correction can be up to 0.5 dex, depending on the T_{eff} .

With these updated parameters the completeness of SWEET-Cat for stars brighter than V magnitude 10 is 85% (77% for stars brighter than 12). For fainter stars it is time expensive to acquire spectra of the quality needed for this method. Moreover, many of the fainter planet host stars have been observed with the *Kepler* space mission, where most stars are faint.

5.3.1 Habitable zone

The habitable zone of a star is at the distance where liquid water may exists. This distance depends on T_{eff} and the luminosity, but also on the planetary atmosphere and its composition. Using [Kopparapu et al. \(2013\)](#) (equation 3 described in [2013](#)) to calculate the inner and upper limits of the habitable zone. The equation is rather simple:

$$d = \sqrt{\frac{L/L_{\odot}}{S_{\text{eff}}}} \text{ AU}, S_{\text{eff}} = S_{\text{eff},\odot} + aT_* + bT_*^2 + cT_*^3 + dT_*^4, \quad (5.2)$$

where $T_* = T_{\text{SI}5780\text{K}}$, and the coefficients can be found in Table 3 in [Kopparapu et al. \(2013\)](#), which depends on the specific model of habitable zone used. Here are used the “Runaway Greenhouse” for the inner limit and “Maximum Greenhouse” for the outer limit of the habitable zone. The equation above is only valid for main sequence stars FGKM, thus only stars with $\log g \geq 4.2 \text{ dex}$ have been included.

It was possible to find three planets within this zone; GJ 785 c, HD 37124 c, and KELT-6 c. These planets does not have known radii, and their minimum masses are $(0.076, 0.652, 3.710)M_{\text{Jupiter}}$, respectively. Thus, it is fair to assume they are all gas planets. All three host stars are metal-poor. A correlation between orbital period and host star metallicity is known (see e.g. [Adibekyan et al., 2013](#)), where metal-poor stars have planets with higher orbital period. It is thus not a surprise that the three planets found in the habitable zone all orbit a metal-poor star. A quick summary of the system is shown in Table [5.3](#).

In Figure [5.2](#) the habitable zone of the stars analysed here are shown along with the location of the planets. The three systems mentioned above are highlighted in the figure.

5.3.2 Changes to planetary parameters

As a results to the analysis above, it is expected that some planetary parameters will change compared with the previous literature values.

Therefore the radius and mass of all the 50 new stars updated in SWEET-Cat were computed using the empirical formula presented in [Torres et al. \(2010\)](#). Some of the stars have radii derived from different methods, usually from isochrones. These radii generally show a good correlation with radii derived from [Torres et al. \(2010\)](#) if the literature parameters of T_{eff} , $\log g$, and $[\text{Fe}/\text{H}]$ are used. However, when comparing with the new radius derived using the parameters presented here, the

Table 5.3: Host star and planetary properties of GJ 785, HD 37124, and KELT-6; all which have an exoplanet in the habitable zone.

Parameter	GJ 785	HD 37124	KELT-6
Stellar parameters			
T_{eff}	$(5087 \pm 48) \text{ K}$	$(5460 \pm 35) \text{ K}$	$(6246 \pm 88) \text{ K}$
$\log g$	$(4.30 \pm 0.10) \text{ dex}$	$(4.26 \pm 0.04) \text{ dex}$	$(4.22 \pm 0.09) \text{ dex}$
$[\text{Fe}/\text{H}]$	$(-0.01 \pm 0.03) \text{ dex}$	$(-0.42 \pm 0.03) \text{ dex}$	$(-0.22 \pm 0.06) \text{ dex}$
Luminosity	$0.72L_{\odot}$	$1.10L_{\odot}$	$2.70L_{\odot}$
V magnitude	6.13	7.68	10.38
Planetary parameters			
Planet	GJ 785 c	HD 37124 c	KELT-6 c
Period	525 days	885 days	1276 days
Mass	$0.076M_J$	$0.652M_J$	$3.710M_J$
Semi-major axis	1.18 AU	1.71 AU	2.39 AU
Inner HZ limit	0.86 AU	1.04 AU	1.56 AU
Outer HZ limit	1.53 AU	1.84 AU	2.70 AU

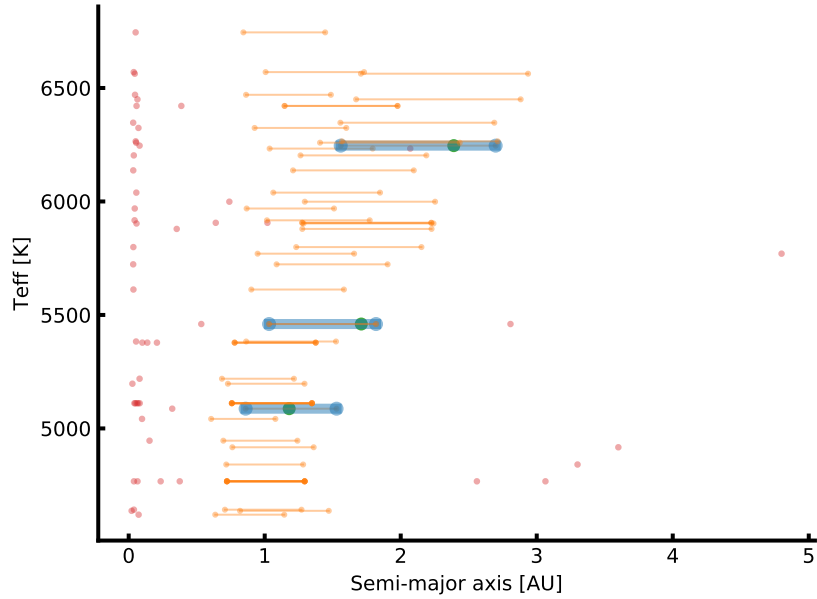


Figure 5.2: The habitable zone for the updated SWEET-Cat stars. The coloured line shows the theoretical habitable zone, while the dots shows the location of the planets in the actual system. The blue lines show the habitable zone of the three stars where a planet is located within it (green points). The red dots and orange lines are systems which does not lie within the habitable zone.

results can differ by up to 65%. This is shown in Figure 5.3 how the radius calculated from [Torres et al. \(2010\)](#) differs between the literature atmospheric parameters and the new homogeneous atmospheric parameters presented here. Note that stellar radii are provided by many of the authors from different discovery papers, but here the atmospheric parameters via the derivation of the stellar radius, as described above, are compared, rather than comparing the stellar radii from different methods.

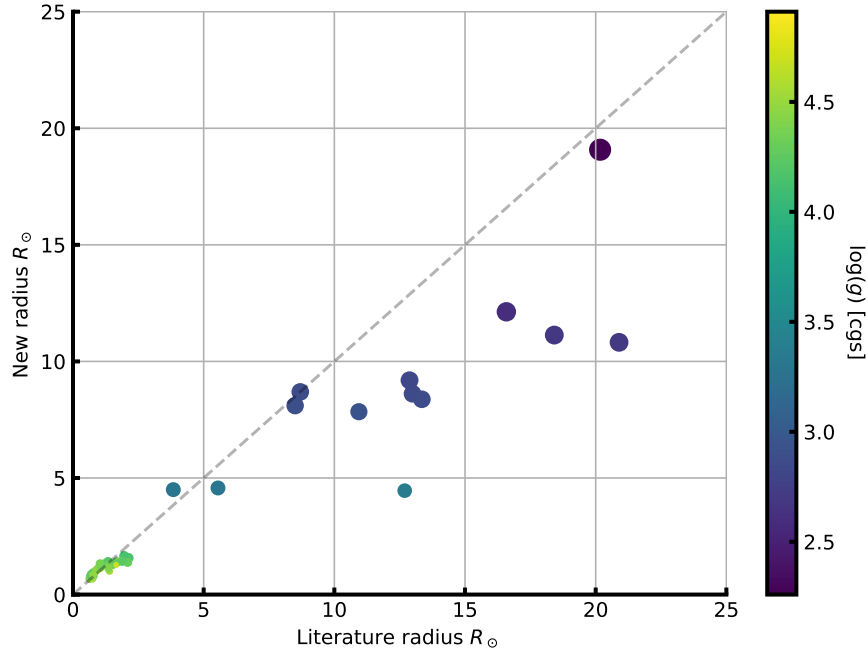


Figure 5.3: Stellar radius on both axes calculated based on [Torres et al. \(2010\)](#). The x-axis shows the stellar radius based on the atmospheric parameters from the literature, while the y-axis indicates the new homogeneous parameters presented here. The colour and size indicate the surface gravity. This clearly shows that the disagreement is biggest for more evolved stars.

In the sections below there follow a discussion of the systems (seven stars, eight exoplanets) where the radius or mass of the stars changes more than 25% and how this influences the planetary parameters. The changes in radius for a star is primarily due to changes in $\log g$, which can be used as an indicator of the evolutionary stage of a star.

The planetary radius, mass, and semi-major axis were re-derived when possible following the three simple scaling relations based on Newton’s law of gravity ([Newton, 1687](#)) for deriving mass and distance and simple geometry for radius (see e.g. [Torres et al., 2008](#))

$$M_{\text{pl,new}} = \left(\frac{M_{*,\text{lit}}}{M_{*,\text{new}}} \right)^{-2/3} M_{\text{pl,lit}} \quad (5.3)$$

$$R_{\text{pl,new}} = \left(\frac{R_{*,\text{lit}}}{R_{*,\text{new}}} \right) R_{\text{pl,lit}} \quad (5.4)$$

$$a_{\text{pl,new}} = \left(\frac{M_{*,\text{lit}}}{M_{*,\text{new}}} \right)^{1/3} a_{\text{pl,lit}}, \quad (5.5)$$

where the subscript “lit” denotes the value from the literature used in the comparison, the subscript “new” indicates the new computed values, the subscript “pl” is short for planet, and the subscript “*” is short for star; M , R , and a are mass, radius, and semi-major axis, respectively. Note that for the literature values, the values reported directly from the literature were used and not the derived radius and mass from [Torres et al. \(2010\)](#). To identify outliers, the radii and masses were compared when derived from [Torres et al. \(2010\)](#) since this is a measure of how the atmospheric parameters have changed.

5.3.2.1 HAT-P-46

HAT-P-46 has two known exoplanets according to [Hartman et al. \(2014\)](#). The outer planet HAT-P-46 c is not transiting, hence the radius is not known for this planet. The results presented above for this star come from UVES/VLT data with a S/N of 208. [Hartman et al. \(2014\)](#) derived the following spectroscopic parameters: $T_{\text{eff}} = (6120 \pm 100) \text{ K}$, $\log g = (4.25 \pm 0.11) \text{ dex}$, and $[\text{Fe}/\text{H}] = (0.30 \pm 0.10) \text{ dex}$. Note that for this star the asteroseismic correction applied (see Section 5.3) results in a corrected $\log g$ below 4.2dex, so the spectroscopic $\log g$ was used for this star.

If mass and radius is derived of HAT-P-46 b with the new parameters, the radius obtained is $R_{\text{pl}} = 0.93R_J$, while [Hartman et al. \(2014\)](#) derived $R_{\text{pl}} = 1.28R_J$. No change in mass is seen ([Hartman et al. 2014](#) found $M_{\text{pl}} = 0.49M_J$); however, there is a decrease in the radius, and this results with a more dense planet, $\rho_{\text{pl}} = 0.76 \text{ g/cm}^3$ from $\rho_{\text{pl}} = (0.28 \pm 0.10) \text{ g/cm}^3$.

Only the minimum mass is known for the secondary companions, as it does not transit HAT-P-46 seen from Earth. With the derived parameters here, the minimum mass is $M \sin i_{\text{pl}} = 1.97M_J$, where [Hartman et al. \(2014\)](#) presented $M \sin i_{\text{pl}} = 2.00M_J$, so a very small change, as expected.

5.3.2.2 HD 120084

The exoplanet orbiting this star with a period of 2082 days and a quite eccentric orbit at 0.66 was discovered by [Sato et al. \(2013\)](#). The atmospheric parameters were derived by [Takeda et al. \(2008\)](#) using a similar method to that described here. The quality of the spectra they analysed, however, were not as high as those used here. Using the HIDES spectrograph at the 188 cm reflector at NAOJ, [Takeda et al. \(2008\)](#) reported an average S/N for their sample of 100-300 objects at a resolving power of 67 000. The spectrum used here is from ESPaDOnS with a resolving power of 81 000, and with a S/N for this star at 850. With the new parameters obtained, there is a slight decrease in stellar mass for the star at $1.93M_{\odot}$ compared to $2.39M_{\odot}$ obtained by [Takeda et al. \(2008\)](#), hence the minimum planetary mass is also slightly lower, from $m_{\text{pl}} \sin i = 4.5M_J$ to $m_{\text{pl}} \sin i = 3.9M_J$. The stellar radius decrease by 28%, from $9.12R_{\odot}$ to $7.81R_{\odot}$. Since there are no observations of the planet transiting, the planetary radius has not been computed.

5.3.2.3 HD 233604

HD 233604 b was discovered by [Nowak et al. \(2013\)](#), while the stellar atmospheric parameters of the star were derived by [Zieliński et al. \(2012\)](#), who used the same method as described here using the HRS spectrograph at HET with a resolving power of 60 000 with a typical S/N at 200-250. For the analysis presented here, a spectrum from the FIES spectrograph was used with a slightly higher resolution at 67 000, and similar but also slightly higher S/N at 320 for this star.

This planet is in a very close orbit with a semi-major axis of $\sim 15R_*$ (R_* is the stellar radius) using the parameters from [Nowak et al. \(2013\)](#). Using the updated parameters presented in this paper the stellar mass increase slightly from $1.5M_{\odot}$ to $1.9M_{\odot}$, and a decrease in stellar radius from $10.5R_{\odot}$ to $8.6R_{\odot}$. This increases the semi-major axis to $\sim 21R_*$. We note that the correct stellar radii are used to describe the semi-major axis in both cases. The increase in stellar mass leads to an increase in the minimum planetary mass, from $m_{\text{pl}} \sin i = 6.58M_J$ to $m_{\text{pl}} \sin i = 7.79M_J$.

Moreover, [Nowak et al. \(2013\)](#) found a high Li abundance at $A(\text{Li})_{\text{LTE}} = (1.400 \pm 0.042)$ dex for this star and speculated that this star might have engulfed a planet. A more likely explanation is that this star has not yet reached the first dredge-up process ([Nowak et al., 2013](#)). In the analysis here a much lower value is found, $A(\text{Li})_{\text{LTE}} = 0.92$ dex, and hence the star is not believed to be Li rich. The Li abundance found here is in excellent agreement with [Adamów et al. \(2014\)](#). Even applying a NLTE correction, as was done in [Adamów et al. \(2014\)](#) ($A(\text{Li})_{\text{NLTE}} = 1.08$), this star is not Li rich.

5.3.2.4 HD 5583

This exoplanet was discovered by [Niedzielski et al. \(2016\)](#) with an orbital period of 139 days around a K giant. This exoplanet was discovered with the radial velocity technique, and the planetary radius is not known. The stellar parameters were derived in a similar manner to that presented here (see [Niedzielski et al., 2016](#), and references therein); the biggest disagreement is in the surface gravity. Here was derived a $\log g$ that is higher by 0.34 dex, which gives a stellar radius that is smaller by 37%. The derived mass is 15% higher, which in turn increases the minimum planetary mass from $m_{\text{pl}} \sin i = 5.78 M_J$ to $m_{\text{pl}} \sin i = 8.63 M_J$. Even with the increase in mass, it is still within the planetary regime for most inclinations, as was noted by [Niedzielski et al. \(2016\)](#).

5.3.2.5 HD 81688

This exoplanet was discovered by [Sato et al. \(2008\)](#) with the RV method. The host star is a metal-poor K giant. The atmospheric parameters presented in [Sato et al. \(2008\)](#) are obtained via the same method as presented here, and the agreement is quite good. Once again the big disagreement is in the surface gravity: Here was obtained 0.48 dex higher. Even though the stellar atmospheric parameters, and hence the planetary parameters, do change, the radius and mass derived are not far from the values presented in the paper by [Sato et al. \(2008\)](#). This is a case where the star was marked as an outlier, due to the comparison between the radius and mass derived from [Torres et al. \(2010\)](#).

The new stellar mass is the same as before, $2.1 M_{\odot}$. The stellar radius changed from $13.0 R_{\odot}$ to $10.8 R_{\odot}$. Since a transit of this star has not been observed and the stellar mass remains the same, there is no change in the planetary parameters.

It is worth noting that this system is in an interesting configuration with a very close orbit around an evolved star. This system, among others, has been the subject of work on planet engulfment (see e.g. [Kunitomo et al., 2011](#)).

5.3.2.6 HIP 107773

The planetary companion was presented in [Jones et al. \(2015\)](#) as an exoplanet around an intermediate-mass evolved star. The stellar parameters were obtained from the analysis by [Jones et al. \(2011\)](#) using the same method as presented here, but with a different line list, which might lead to some disagreements. A higher $\log g$ (2.83 dex compared to 2.60 dex) was derived here, thus the star is slightly smaller with $11.6 R_{\odot}$ to $9.2 R_{\odot}$ and $2.4 M_{\odot}$ to $2.1 M_{\odot}$ for radius and mass of the star, respectively. The other atmospheric parameters are very similar to those derived by [Jones et al. \(2011\)](#). This leads to a reduced minimum mass of the planetary companion from $m \sin i = 1.98 M_J$ to $m \sin i = 1.78 M_J$. The planetary radius has not been measured.

5.3.2.7 WASP-97

The exoplanet orbiting WASP-97 was discovered by [Hellier et al. \(2014\)](#). The host star parameters were derived using a similar method to that described here after co-adding several spectra from the CORALIE spectrograph. They reach a S/N of 100 with a spectral resolution of 50 000. The parameters presented here come from the UVES spectrograph with a S/N of more than 200.

The parameters do not change much for this planet. The minimum planetary mass changes from $m_{\text{pl}} \sin i = 1.32M_J$ to $m_{\text{pl}} \sin i = 1.37M_J$ and the radius from $1.13R_J$ to $1.42R_J$. This affects the density quite strongly; it changes from 1.13 g/cm^3 to 0.59 g/cm^3 . This exoplanet is then in the same category as Saturn; its density is lower than water, but it is slightly larger than Jupiter.

5.3.2.8 ω Serpentis (ome Ser)

The exoplanet orbiting this star with a period of 277 days and an eccentric orbit at 0.11 was also presented by [Sato et al. \(2013\)](#). The atmospheric parameters were derived in the same way as for HD 120084. Data from FIES with a resolving power of 67 000 was used, and with a S/N for this star of 1168. With the new parameters a slightly higher stellar mass for the star is obtained at $2.19M_{\odot}$ compared to the value of $2.17M_{\odot}$ obtained by [Takeda et al. \(2008\)](#). This change is not significant enough to change the minimum planetary mass at $m_{\text{pl}} \sin i = 1.7M_J$. The stellar radius decreases by more than one solar radius, from $12.3R_{\odot}$ to $11.1R_{\odot}$. However, since there are no observations of transiting exoplanets, any change in planetary radius cannot be detected.

5.3.2.9 \omicron Ursa Major (omi UMa)

omi UMa b was discovered by [Sato et al. \(2012\)](#) using the RV method. The stellar parameters are from [Takeda et al. \(2008\)](#), as discussed above. The spectrum used for this star is from ESPaDOnS with a S/N of more than 500 compared to the value of 100-300 reached for the large sample presented in [Takeda et al. \(2008\)](#). The luminosity and mass for omi UMa were obtained from theoretical evolutionary tracks (see [Sato et al., 2012](#), and references therein). The radius was then estimated using the Stefan-Boltzmann relationship, using the measured luminosity and T_{eff} .

The parameters presented here mainly differ in the surface gravity: here it is 0.72 dex higher at $\log g = 3.36$. This leads to a big change in stellar mass and radius from $3.1M_{\odot}$ to $1.6M_{\odot}$ and $14.1R_{\odot}$ to $4.5R_{\odot}$, respectively. [Sato et al. \(2012\)](#) have reported that omi UMa b is the first planet candidate around a star more massive than $3M_{\odot}$, which is not supported by the results presented here. With these updated results, the minimum mass of the planet is now $m \sin i = 2.7M_J$, whereas previously it was $m \sin i = 4.1M_J$ ([Sato et al., 2012](#)). The exoplanet is not reported to transit, as seen from Earth, so the radius for this exoplanet is not known, which would have changed a great deal with these new results.

5.4 Discovering two giant planet populations

SWEET-Cat was recently combined with planetary masses to see two distinctive populations for giant planets by [Santos et al. \(2017\)](#). This can be seen in the mass histogram in Figure 5.4 for the full sample of giant planets, with masses higher than 1 Jupiter mass and lower than 20 Jupiter masses, and

for a sample constrained by: $4000\text{ K} \leq T_{\text{eff}} \leq 6500\text{ K}$ in order to have reliably atmospheric parameters from spectroscopic data, orbital periods above 10 days to avoid hot jupiters whose formation and migration process is debated (Ngo et al., 2016, see e.g.), orbital periods below 5 years to allow for the sample to be reasonable complete. Last only stars brighter than 13 magnitude were included to ensure that the planetary masses can have been derived with reasonable confidence using the radial velocities.

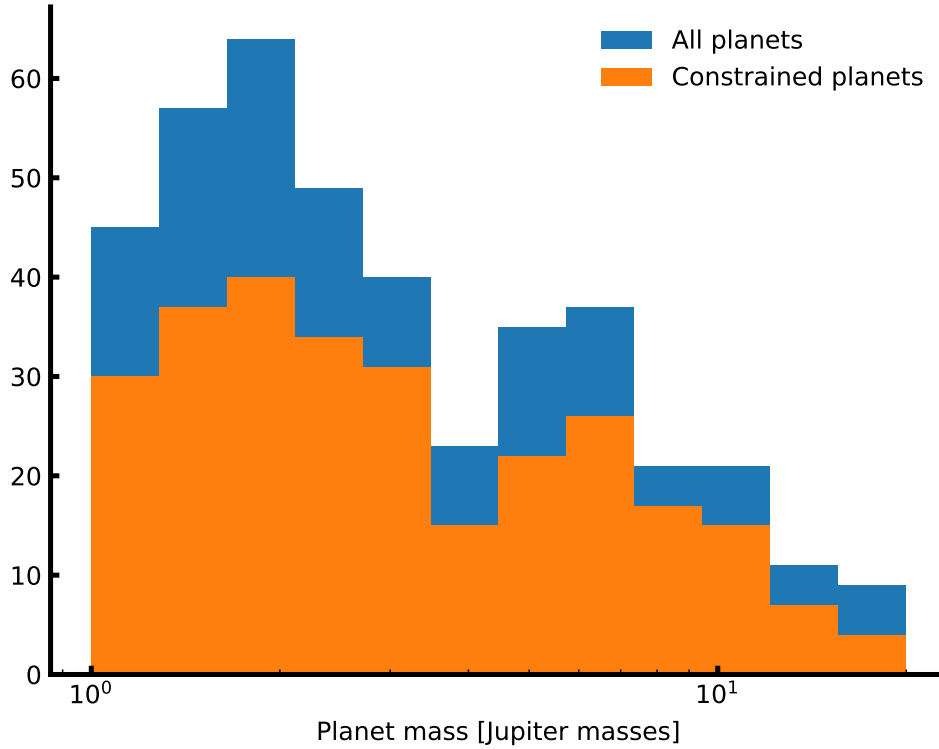


Figure 5.4: Giant planet masses for the full sample and constrained sample (see text for details). This study was performed by Santos et al. (2017) to distinct two giant planet populations.

By separating the distribution into two at $4M_{Jup}$, it can be shown (see Santos et al., 2017, for details) that the stars hosting the more massive giant planets are in average more metal-poor compared to the stars hosting the lower mass giant planets. This suggest two different stellar populations forming giant planets.

5.5 Future work

Table 1: Derived parameters for the 50 stars in our sample. The S/N was measured by ARES.

Star	T_{eff} (K)	$\log g$ (dex)	[Fe / H] (dex)	ξ_{micro} (km/s)	ξ_{micro} fixed?	Instrument	S/N
BD -11 4672	4553 ± 75	4.87 ± 0.51	-0.30 ± 0.02	0.14 ± 0.07	yes	FIES	487
BD +49 828	5015 ± 36	$2.87 \pm 0.09^{\text{a}}$	-0.01 ± 0.03	1.48 ± 0.04	no	FIES	567
GJ 785	5087 ± 48	4.42 ± 0.10	-0.01 ± 0.03	0.69 ± 0.10	no	HARPS	801
HATS-1	5969 ± 46	4.39 ± 0.06	-0.04 ± 0.04	1.06 ± 0.08	no	UVES	155
HATS-5	5383 ± 91	4.41 ± 0.22	0.08 ± 0.06	0.91 ± 0.14	no	UVES	158
HAT-P-12	4642 ± 106	4.53 ± 0.27	-0.26 ± 0.06	0.28 ± 0.63	no	FIES	185
HAT-P-24	6470 ± 181	4.33 ± 0.27	-0.41 ± 0.10	1.40 ± 0.03	yes	UVES	158
HAT-P-39	6745 ± 236	4.39 ± 0.47	-0.21 ± 0.12	1.53 ± 0.04	yes	UVES	127
HAT-P-42	5903 ± 66	$4.29 \pm 0.10^{\text{a}}$	0.34 ± 0.05	1.19 ± 0.08	no	UVES	130
HAT-P-46	6421 ± 121	$4.53 \pm 0.14^{\text{a}}$	0.16 ± 0.09	1.67 ± 0.18	no	UVES	208
HD 120084	4969 ± 40	$2.94 \pm 0.14^{\text{a}}$	0.12 ± 0.03	1.41 ± 0.04	no	ESPaDOnS	852
HD 192263	4946 ± 46	4.61 ± 0.14	-0.05 ± 0.02	0.66 ± 0.12	no	HARPS	415
HD 219134	4767 ± 70	4.57 ± 0.17	0.00 ± 0.04	0.59 ± 0.24	no	ESPaDOnS	725
HD 220842	5999 ± 39	$4.30 \pm 0.06^{\text{a}}$	-0.08 ± 0.03	1.21 ± 0.05	no	FIES	459
HD 233604	4954 ± 46	$2.86 \pm 0.11^{\text{a}}$	-0.14 ± 0.04	1.61 ± 0.05	no	FIES	314
HD 283668	4841 ± 73	4.51 ± 0.18	-0.74 ± 0.04	0.16 ± 0.61	no	FIES	592
HD 285507	4620 ± 126	4.72 ± 0.61	0.04 ± 0.06	0.74 ± 0.43	no	UVES	239
HD 5583	4986 ± 35	$2.87 \pm 0.09^{\text{a}}$	-0.35 ± 0.03	1.62 ± 0.04	no	FIES	933
HD 81688	4903 ± 21	$2.70 \pm 0.05^{\text{a}}$	-0.21 ± 0.02	1.54 ± 0.02	no	^b	1350, 860

Star	T_{eff} (K)	$\log g$ (dex)	[Fe / H] (dex)	ξ_{micro} (km/s)	ξ_{micro} fixed?	Instrument	S/N
HD 82886	5123 ± 18	$3.30 \pm 0.04^{\text{a}}$	-0.25 ± 0.01	1.16 ± 0.02	no	^c	1198,1294
HD 87883	4917 ± 68	4.53 ± 0.19	0.02 ± 0.03	0.46 ± 0.21	no	ESPaDOnS	753
HIP 107773	4957 ± 49	$2.83 \pm 0.09^{\text{a}}$	0.04 ± 0.04	1.49 ± 0.05	no	UVES	218
HIP 11915	5770 ± 14	4.33 ± 0.03	-0.06 ± 0.01	0.95 ± 0.02	no	HARPS	709
HIP 116454	5042 ± 72	4.69 ± 0.15	-0.16 ± 0.03	0.71 ± 0.17	no	UVES	412
HR 228	5042 ± 42	$3.30 \pm 0.09^{\text{a}}$	0.07 ± 0.03	1.14 ± 0.04	no	UVES	400
KELT-6	6246 ± 88	$4.22 \pm 0.09^{\text{a}}$	-0.22 ± 0.06	1.66 ± 0.13	no	FIES	374
Kepler-37	5378 ± 53	4.47 ± 0.12	-0.23 ± 0.04	0.58 ± 0.13	no	FIES	205
Kepler-444	5111 ± 43	4.50 ± 0.13	-0.51 ± 0.03	0.37 ± 0.15	no	FIES	675
mu Leo	4605 ± 94	$2.61 \pm 0.26^{\text{a}}$	0.25 ± 0.06	1.64 ± 0.11	no	ESPaDOnS	354
ome Ser	4928 ± 35	$2.69 \pm 0.06^{\text{a}}$	-0.11 ± 0.03	1.55 ± 0.04	no	FIES	1168
omi UMa	5499 ± 52	$3.36 \pm 0.07^{\text{a}}$	-0.01 ± 0.05	1.98 ± 0.06	no	ESPaDOnS	527
Qatar-2	4637 ± 316	4.53 ± 0.62	0.09 ± 0.17	0.63 ± 0.83	no	UVES	97
SAND364	4457 ± 104	$2.26 \pm 0.20^{\text{a}}$	-0.04 ± 0.06	1.60 ± 0.11	no	UVES	220
TYC+1422-614-1	4908 ± 41	$2.90 \pm 0.12^{\text{a}}$	-0.07 ± 0.03	1.57 ± 0.05	no	FIES	506
WASP-37	5917 ± 72	4.25 ± 0.15	-0.23 ± 0.05	0.59 ± 0.13	no	FIES	232
WASP-44	5612 ± 80	4.39 ± 0.30	0.17 ± 0.06	1.32 ± 0.13	no	UVES	125
WASP-52	5197 ± 83	4.55 ± 0.30	0.15 ± 0.05	1.16 ± 0.14	no	UVES	125
WASP-58	6039 ± 55	4.23 ± 0.10	-0.09 ± 0.04	1.12 ± 0.08	no	FIES	310
WASP-61	6265 ± 168	$4.21 \pm 0.21^{\text{a}}$	-0.38 ± 0.11	1.44 ± 0.02	yes	UVES	163

Star	T_{eff} (K)	$\log g$ (dex)	[Fe / H] (dex)	ξ_{micro} (km/s)	ξ_{micro} fixed?	Instrument	S/N
WASP-72	6570 ± 85	4.25 ± 0.13	0.15 ± 0.06	2.30 ± 0.15	no	UVES	174
WASP-73	6203 ± 32	$4.16 \pm 0.06^{\text{a}}$	0.20 ± 0.02	1.66 ± 0.04	np	^d	193,231
WASP-75	6203 ± 46	$4.42 \pm 0.22^{\text{a}}$	0.24 ± 0.03	1.45 ± 0.06	no	UVES	189
WASP-76	6347 ± 52	$4.29 \pm 0.08^{\text{a}}$	0.36 ± 0.04	1.73 ± 0.06	no	UVES	165
WASP-82	6563 ± 55	$4.29 \pm 0.10^{\text{a}}$	0.18 ± 0.04	1.93 ± 0.08	no	UVES	239
WASP-88	6450 ± 61	$4.24 \pm 0.06^{\text{a}}$	0.03 ± 0.04	1.79 ± 0.09	no	UVES	174
WASP-94 A	6259 ± 34	$4.34 \pm 0.07^{\text{a}}$	0.35 ± 0.03	1.50 ± 0.04	no	UVES	356
WASP-94 B	6137 ± 21	$4.42 \pm 0.05^{\text{a}}$	0.33 ± 0.02	1.29 ± 0.03	no	UVES	397
WASP-95	5799 ± 31	$4.29 \pm 0.05^{\text{a}}$	0.22 ± 0.03	1.18 ± 0.04	no	UVES	247
WASP-97	5723 ± 52	4.24 ± 0.07	0.31 ± 0.04	1.03 ± 0.08	no	UVES	219
WASP-99	6324 ± 89	4.34 ± 0.12	0.27 ± 0.06	1.83 ± 0.12	no	UVES	249
WASP-100	6853 ± 209	$4.15 \pm 0.26^{\text{a}}$	-0.30 ± 0.12	1.87 ± 0.02	yes	UVES	166

^a Spectroscopic $\log g$.

^b Weighted average of ESPaDoNS and FIES results. The parameters are (FIES in parantheses): $T_{\text{eff}} = 4870(4934) \pm 30(29)$, $\log g = 2.50(2.73) \pm 0.14(0.05)$, $[\text{Fe} / \text{H}] = -0.26(-0.19) \pm 0.03(0.02)$, and $\xi_{\text{micro}} = 1.50(1.59) \pm 0.03(0.03)$.

^c Weighted average of ESPaDoNS and FIES results. The parameters are (FIES in parantheses): $T_{\text{eff}} = 5124(5121) \pm 22(29)$, $\log g = 3.30(3.31) \pm 0.05(0.07)$, $[\text{Fe} / \text{H}] = -0.25(-0.24) \pm 0.02(0.02)$, and $\xi_{\text{micro}} = 1.15(1.17) \pm 0.03(0.04)$.

^d Weighted average of UVES and FEROS results. The parameters are (FEROS in parantheses): $T_{\text{eff}} = 6313(6162) \pm 61(37)$, $\log g = 4.26(4.14) \pm 0.15(0.06)$, $[\text{Fe} / \text{H}] = 0.22(0.19) \pm 0.04(0.03)$, and $\xi_{\text{micro}} = 1.85(1.61) \pm 0.08(0.04)$.

Bibliography

- Adamów, M., Niedzielski, A., Villaver, E., Wolszczan, A., and Nowak, G.: 2014, *A&A* **569**, A55
- Adibekyan, V. Z., Benamati, L., Santos, N. C., Alves, S., Lovis, C., Udry, S., Israelian, G., Sousa, S. G., Tsantaki, M., Mortier, A., Sozzetti, A., and De Medeiros, J. R.: 2015, *MNRAS* **450**, 1900
- Adibekyan, V. Z., Figueira, P., Santos, N. C., Mortier, A., Mordasini, C., Delgado Mena, E., Sousa, S. G., Correia, A. C. M., Israelian, G., and Oshagh, M.: 2013, *A&A* **560**, A51
- Aerts, C., Christensen-Dalsgaard, J., and Kurtz, D. W.: 2010, *Asteroseismology*, Springer-Verlag
- Ammler-von Eiff, M., Santos, N. C., Sousa, S. G., Fernandes, J., Guillot, T., Israelian, G., Mayor, M., and Melo, C.: 2009, *A&A* **507**, 523
- Andreasen, D. T., Sousa, S. G., Delgado Mena, E., Santos, N. C., Lebzelter, T., Mucciarelli, A., and Neil, J. J.: 2017a, *A&A* **585**, A143
- Andreasen, D. T., Sousa, S. G., Delgado Mena, E., Santos, N. C., Tsantaki, M., Rojas-Ayala, B., and Neves, V.: 2016, *A&A* **585**, A143
- Andreasen, D. T., Sousa, S. G., Tsantaki, M., Teixeira, G. D. C., Mortier, A., Santos, N. C., Suárez-Andrés, L., Delgado Mena, E., and Ferreira, A. C. S.: 2017b, *A&A* **600**, A69
- Artigau, É., Kouach, D., Donati, J.-F., Doyon, R., Delfosse, X., Baratchart, S., Lacombe, M., Moutou, C., Rabou, P., Parès, L. P., Mischeau, Y., Thibault, S., Reshetov, V. A., Dubois, B., Hernandez, O., Vallée, P., Wang, S.-Y., Dolon, F., Pepe, F. A., Bouchy, F., Striebig, N., Hénault, F., Loop, D., Saddlemyer, L., Barrick, G., Vermeulen, T., Dupieux, M., Hébrard, G., Boisse, I., Martioli, E., Alencar, S. H. P., do Nascimento, J.-D., and Figueira, P.: 2014, in *Society of Photo-Optical Instrumentation Engineers (SPIE) Conference Series*, Vol. 9147 of *Society of Photo-Optical Instrumentation Engineers (SPIE) Conference Series*, p. 15
- Balachandran, S.: 1990, *ApJ* **354**, 310
- Baraffe, I., Homeier, D., Allard, F., and Chabrier, G.: 2015, *A&A* **577**, A42
- Bedding, T. R., Mosser, B., Huber, D., Montalbán, J., Beck, P., Christensen-Dalsgaard, J., Elsworth, Y. P., García, R. A., Miglio, A., Stello, D., White, T. R., De Ridder, J., Hekker, S., Aerts, C., Barban, C., Belkacem, K., Broomhall, A.-M., Brown, T. M., Buzasi, D. L., Carrier, F., Chaplin, W. J., di Mauro, M. P., Dupret, M.-A., Frandsen, S., Gilliland, R. L., Goupil, M.-J., Jenkins, J. M., Kallinger, T., Kawaler, S., Kjeldsen, H., Mathur, S., Noels, A., Silva Aguirre, V., and Ventura, P.: 2011, *Nature* **471**, 608
- Bensby, T., Feltzing, S., and Oey, M. S.: 2014, *A&A* **562**, A71

- Bertaux, J. L., Lallement, R., Ferron, S., Boonne, C., and Bodichon, R.: 2014, *A&A* **564**, A46
- Blackwell, D. E. and Shallis, M. J.: 1977, *MNRAS* **180**, 177
- Bochanski, J. J., Hawley, S. L., Covey, K. R., West, A. A., Reid, I. N., Golimowski, D. A., and Ivezić, Ž.: 2010, *AJ* **139**, 2679
- Boyajian, T. S., von Braun, K., van Belle, G., McAlister, H. A., ten Brummelaar, T. A., Kane, S. R., Muirhead, P. S., Jones, J., White, R., Schaefer, G., Ciardi, D., Henry, T., López-Morales, M., Ridgway, S., Gies, D., Jao, W.-C., Rojas-Ayala, B., Parks, J. R., Sturmann, L., Sturmann, J., Turner, N. H., Farrington, C., Goldfinger, P. J., and Berger, D. H.: 2012, *ApJ* **757**, 112
- Casagrande, L., Portinari, L., and Flynn, C.: 2006, *MNRAS* **373**, 13
- Casagrande, L., Ramírez, I., Meléndez, J., Bessell, M., and Asplund, M.: 2010, *A&A* **512**, A54
- Cayrel, R.: 1988, in G. Cayrel de Strobel and M. Spite (eds.), *The Impact of Very High S/N Spectroscopy on Stellar Physics*, Vol. 132 of *IAU Symposium*, p. 345
- Chaplin, W. J., Kjeldsen, H., Christensen-Dalsgaard, J., Basu, S., Miglio, A., Appourchaux, T., Bedding, T. R., Elsworth, Y., García, R. A., Gilliland, R. L., Girardi, L., Houdek, G., Karoff, C., Kawaler, S. D., Metcalfe, T. S., Molenda-Żakowicz, J., Monteiro, M. J. P. F. G., Thompson, M. J., Verner, G. A., Ballot, J., Bonanno, A., Brandão, I. M., Broomhall, A.-M., Bruntt, H., Campante, T. L., Corsaro, E., Creevey, O. L., Doğan, G., Esch, L., Gai, N., Gaulme, P., Hale, S. J., Handberg, R., Hekker, S., Huber, D., Jiménez, A., Mathur, S., Mazumdar, A., Mosser, B., New, R., Pinsonneault, M. H., Pricopi, D., Quirion, P.-O., Régulo, C., Salabert, D., Serenelli, A. M., Silva Aguirre, V., Sousa, S. G., Stello, D., Stevens, I. R., Suran, M. D., Uytterhoeven, K., White, T. R., Borucki, W. J., Brown, T. M., Jenkins, J. M., Kinemuchi, K., Van Cleve, J., and Klaus, T. C.: 2011, *Science* **332**, 213
- Christensen-Dalsgaard, J., Kjeldsen, H., Brown, T. M., Gilliland, R. L., Arentoft, T., Frandsen, S., Quirion, P.-O., Borucki, W. J., Koch, D., and Jenkins, J. M.: 2010, *ApJL* **713**, L164
- Conod, U., Blind, N., Wildi, F., and Pepe, F.: 2016, in *Society of Photo-Optical Instrumentation Engineers (SPIE) Conference Series*, Vol. 9909 of *Proceedings of the SPIE*, p. 990941
- Czekala, I., Andrews, S. M., Mandel, K. S., Hogg, D. W., and Green, G. M.: 2015, *ApJ* **812**, 128
- Dekker, H., D’Odorico, S., Kaufer, A., Delabre, B., and Kotzlowski, H.: 2000, in M. Iye and A. F. Moorwood (eds.), *Optical and IR Telescope Instrumentation and Detectors*, Vol. 4008 of *Proceedings of the SPIE*, pp 534–545
- Delfosse, X., Donati, J.-F., Kouach, D., Hébrard, G., Doyon, R., Artigau, E., Bouchy, F., Boisse, I., Brun, A. S., Hennebelle, P., Widemann, T., Bouvier, J., Bonfils, X., Morin, J., Moutou, C., Pepe, F., Udry, S., do Nascimento, J.-D., Alencar, S. H. P., Castilho, B. V., Martioli, E., Wang, S. Y., Figueira, P., and Santos, N. C.: 2013, in L. Cambresy, F. Martins, E. Nuss, and A. Palacios (eds.), *SF2A-2013: Proceedings of the Annual meeting of the French Society of Astronomy and Astrophysics*, pp 497–508
- Donati, J.-F.: 2003, in J. Trujillo-Bueno and J. Sanchez Almeida (eds.), *Solar Polarization*, Vol. 307 of *Astronomical Society of the Pacific Conference Series*, p. 41
- Dotter, A., Chaboyer, B., Jevremović, D., Kostov, V., Baron, E., and Ferguson, J. W.: 2008, *ApJS* **178**, 89

- Ducati, J. R.: 2002, *VizieR Online Data Catalog* 2237
- Favata, F., Micela, G., and Sciortino, S.: 1997, *A&A* **323**, 809
- Follert, R., Dorn, R. J., Oliva, E., Lizon, J. L., Hatzes, A., Piskunov, N., Reiners, A., Seemann, U., Stempels, E., Heiter, U., Marquart, T., Lockhart, M., Anglada-Escude, G., Löwinger, T., Baade, D., Grunhut, J., Bristow, P., Klein, B., Jung, Y., Ives, D. J., Kerber, F., Pozna, E., Paufigue, J., Kaeufl, H. U., Origlia, L., Valenti, E., Gojak, D., Hilker, M., Pasquini, L., Smette, A., and Smoker, J.: 2014, in *Society of Photo-Optical Instrumentation Engineers (SPIE) Conference Series*, Vol. 9147 of *Society of Photo-Optical Instrumentation Engineers (SPIE) Conference Series*, p. 19
- Frandsen, S. and Lindberg, B.: 1999, in H. Karttunen and V. Pirola (eds.), *Astrophysics with the NOT*, p. 71
- Girardi, L., Bressan, A., Bertelli, G., and Chiosi, C.: 2000, *A&A Supp.* **141**, 371
- Gonzalez, G., Carlson, M. K., and Tobin, R. W.: 2010, *MNRAS* **403**, 1368
- Gonzalez, G. and Laws, C.: 2000, *AJ* **119**, 390
- Gray, D. F.: 2005, *The Observation and Analysis of Stellar Photospheres*, 3rd ed.
- Griffin, R. and Griffin, R.: 1967, *MNRAS* **137**, 253
- Grundahl, F., Fredslund Andersen, M., Christensen-Dalsgaard, J., Antoci, V., Kjeldsen, H., Handberg, R., Houdek, G., Bedding, T. R., Pallé, P. L., Jessen-Hansen, J., Silva Aguirre, V., White, T. R., Frandsen, S., Albrecht, S., Andersen, M. I., Arentoft, T., Brogaard, K., Chaplin, W. J., Harpsøe, K., Jørgensen, U. G., Karovicova, I., Karoff, C., Kjærgaard Rasmussen, P., Lund, M. N., Sloth Lundkvist, M., Skottfelt, J., Norup Sørensen, A., Tronsgaard, R., and Weiss, E.: 2017, *ApJ* **836**, 142
- Gustafsson, B., Edvardsson, B., Eriksson, K., Jørgensen, U. G., Nordlund, Å., and Plez, B.: 2008, *A&A* **486**, 951
- Hartman, J. D., Bakos, G. Á., Torres, G., Kovács, G., Johnson, J. A., Howard, A. W., Marcy, G. W., Latham, D. W., Bieryla, A., Buchhave, L. A., Bhatti, W., Béky, B., Csubry, Z., Penev, K., de Val-Borro, M., Noyes, R. W., Fischer, D. A., Esquerdo, G. A., Everett, M., Szklenár, T., Zhou, G., Bayliss, D., Shporer, A., Fulton, B. J., Sanchis-Ojeda, R., Falco, E., Lázár, J., Papp, I., and Sári, P.: 2014, *AJ* **147**, 128
- Hellier, C., Anderson, D. R., Cameron, A. C., Delrez, L., Gillon, M., Jehin, E., Lendl, M., Maxted, P. F. L., Pepe, F., Pollacco, D., Queloz, D., Ségransan, D., Smalley, B., Smith, A. M. S., Southworth, J., Triaud, A. H. M. J., Udry, S., and West, R. G.: 2014, *MNRAS* **440**, 1982
- Hinkel, N. R., Young, P. A., Pagano, M. D., Desch, S. J., Anbar, A. D., Adibekyan, V., Blanco-Cuaresma, S., Carlberg, J. K., Delgado Mena, E., Liu, F., Nordlander, T., Sousa, S. G., Korn, A., Gruyters, P., Heiter, U., Jofré, P., Santos, N. C., and Soubiran, C.: 2016, *ApJS* **226**, 4
- Hinkle, K., Wallace, L., and Livingston, W.: 1995a, *Publications of the ASP* **107**, 1042
- Hinkle, K. H., Wallace, L., and Livingston, W.: 1995b, in A. J. Sauval, R. Blomme, and N. Grevesse (eds.), *Laboratory and Astronomical High Resolution Spectra*, Vol. 81 of *Astronomical Society of the Pacific Conference Series*, p. 66

- Huber, D., Silva Aguirre, V., Matthews, J. M., Pinsonneault, M. H., Gaidos, E., García, R. A., Hekker, S., Mathur, S., Mosser, B., Torres, G., Bastien, F. A., Basu, S., Bedding, T. R., Chaplin, W. J., Demory, B.-O., Fleming, S. W., Guo, Z., Mann, A. W., Rowe, J. F., Serenelli, A. M., Smith, M. A., and Stello, D.: 2014, *ApJS* **211**, 2
- Husser, T.-O., Wende-von Berg, S., Dreizler, S., Homeier, D., Reiners, A., Barman, T., and Hauschildt, P. H.: 2013, *A&A* **553**, A6
- Jofré, P., Heiter, U., Soubiran, C., Blanco-Cuaresma, S., Worley, C. C., Pancino, E., Cantat-Gaudin, T., Magrini, L., Bergemann, M., González Hernández, J. I., Hill, V., Lardo, C., de Laverny, P., Lind, K., Masseron, T., Montes, D., Mucciarelli, A., Nordlander, T., Recio Blanco, A., Sobeck, J., Sordo, R., Sousa, S. G., Tabernero, H., Vallenari, A., and Van Eck, S.: 2014, *A&A* **564**, A133
- Jones, M. I., Jenkins, J. S., Rojo, P., and Melo, C. H. F.: 2011, *A&A* **536**, A71
- Jones, M. I., Jenkins, J. S., Rojo, P., Olivares, F., and Melo, C. H. F.: 2015, *A&A* **580**, A14
- Kaufer, A., Stahl, O., Tubbesing, S., Nørregaard, P., Avila, G., Francois, P., Pasquini, L., and Pizzella, A.: 1999, *The Messenger* **95**, 8
- Kippenhahn, R. and Weigert, A.: 1994, *Stellar Structure and Evolution*, Springer-Verlag
- Kjeldsen, H. and Bedding, T. R.: 1995, *A&A* **293**, 87
- Kopparapu, R. K., Ramirez, R., Kasting, J. F., Eymet, V., Robinson, T. D., Mahadevan, S., Terrien, R. C., Domagal-Goldman, S., Meadows, V., and Deshpande, R.: 2013, *ApJ* **765**, 131
- Kotani, T., Tamura, M., Suto, H., Nishikawa, J., Sato, B., Aoki, W., Usuda, T., Kurokawa, T., Kashiwagi, K., Nishiyama, S., Ikeda, Y., Hall, D. B., Hodapp, K. W., Hashimoto, J., Morino, J.-I., Okuyama, Y., Tanaka, Y., Suzuki, S., Inoue, S., Kwon, J., Suenaga, T., Oh, D., Baba, H., Narita, N., Kokubo, E., Hayano, Y., Izumiura, H., Kambe, E., Kudo, T., Kusakabe, N., Ikoma, M., Hori, Y., Omiya, M., Genda, H., Fukui, A., Fujii, Y., Guyon, O., Harakawa, H., Hayashi, M., Hidai, M., Hirano, T., Kuzuhara, M., Machida, M., Matsuo, T., Nagata, T., Onuki, H., Ogihara, M., Takami, H., Takato, N., Takahashi, Y. H., Tachinami, C., Terada, H., Kawahara, H., and Yamamuro, T.: 2014, in *Society of Photo-Optical Instrumentation Engineers (SPIE) Conference Series*, Vol. 9147 of *Society of Photo-Optical Instrumentation Engineers (SPIE) Conference Series*, p. 14
- Kunitomo, M., Ikoma, M., Sato, B., Katsuta, Y., and Ida, S.: 2011, *ApJ* **737**, 66
- Kupka, F. G., Ryabchikova, T. A., Piskunov, N. E., Stempels, H. C., and Weiss, W. W.: 2000, *Baltic Astronomy* **9**, 590
- Kurucz, R.: 1993, *ATLAS9 Stellar Atmosphere Programs and 2 km/s grid. Kurucz CD-ROM No. 13. Cambridge, Mass.: Smithsonian Astrophysical Observatory, 1993*. 13
- Lebzelter, T., Heiter, U., Abia, C., Eriksson, K., Ireland, M., Neilson, H., Nowotny, W., Maldonado, J., Merle, T., Peterson, R., Plez, B., Short, C. I., Wahlgren, G. M., Worley, C., Aringer, B., Bladh, S., de Laverny, P., Goswami, A., Mora, A., Norris, R. P., Recio-Blanco, A., Scholz, M., Thévenin, F., Tsuji, T., Kordopatis, G., Montesinos, B., and Wing, R. F.: 2012a, *A&A* **547**, A108
- Lebzelter, T., Seifahrt, A., Uttenthaler, S., Ramsay, S., Hartman, H., Nieva, M.-F., Przybilla, N., Smette, A., Wahlgren, G. M., Wolff, B., Hussain, G. A. J., Käufel, H. U., and Seemann, U.: 2012b, *A&A* **539**, A109

- Lindgren, S., Heiter, U., and Seifahrt, A.: 2016, *A&A* **586**, A100
- Mayor, M., Pepe, F., Queloz, D., Bouchy, F., Rupprecht, G., Lo Curto, G., Avila, G., Benz, W., Bertaux, J.-L., Bonfils, X., Dall, T., Dekker, H., Delabre, B., Eckert, W., Fleury, M., Gilliotte, A., Gojak, D., Guzman, J. C., Kohler, D., Lizon, J.-L., Longinotti, A., Lovis, C., Megevand, D., Pasquini, L., Reyes, J., Sivan, J.-P., Sosnowska, D., Soto, R., Udry, S., van Kesteren, A., Weber, L., and Weilenmann, U.: 2003, *The Messenger* **114**, 20
- McWilliam, A.: 1990, *ApJS* **74**, 1075
- Meléndez, J. and Barbuy, B.: 1999, *ApJS* **124**, 527
- Mortier, A., Santos, N. C., Sousa, S., Israelian, G., Mayor, M., and Udry, S.: 2013a, *A&A* **551**, A112
- Mortier, A., Santos, N. C., Sousa, S. G., Adibekyan, V. Z., Delgado Mena, E., Tsantaki, M., Israelian, G., and Mayor, M.: 2013b, *A&A* **557**, A70
- Mortier, A., Sousa, S. G., Adibekyan, V. Z., Brandão, I. M., and Santos, N. C.: 2014, *A&A* **572**, A95
- Mucciarelli, A., Pancino, E., Lovisi, L., Ferraro, F. R., and Lapenna, E.: 2013, *ApJ* **766**, 78
- Neuforge-Verheecke, C. and Magain, P.: 1997, *A&A* **328**, 261
- Newton, I.: 1687, *Philosophiae Naturalis Principia Mathematica. Auctore Js. Newton*
- Ngo, H., Knutson, H. A., Hinkley, S., Bryan, M., Crepp, J. R., Batygin, K., Crossfield, I., Hansen, B., Howard, A. W., Johnson, J. A., Mawet, D., Morton, T. D., Muirhead, P. S., and Wang, J.: 2016, *ApJ* **827**, 8
- Nicholls, C. P., Lebzelter, T., Smette, A., Wolff, B., Hartman, H., Käuff, H.-U., Przybilla, N., Ramsay, S., Uttenthaler, S., Wahlgren, G. M., Bagnulo, S., Hussain, G. A. J., Nieva, M.-F., Seemann, U., and Seifahrt, A.: 2017, *A&A* **598**, A79
- Niedzielski, A., Villaver, E., Nowak, G., Adamów, M., Kowalik, K., Wolszczan, A., Dekaszyankiewicz, B., Adamczyk, M., and Maciejewski, G.: 2016, *A&A* **588**, A62
- Nowak, G., Niedzielski, A., Wolszczan, A., Adamów, M., and Maciejewski, G.: 2013, *ApJ* **770**, 53
- Önehag, A., Heiter, U., Gustafsson, B., Piskunov, N., Plez, B., and Reiners, A.: 2012, *A&A* **542**, A33
- Origlia, L., Oliva, E., Baffa, C., Falcini, G., Giani, E., Massi, F., Montegriffo, P., Sanna, N., Scuderi, S., Sozzi, M., Tozzi, A., Carleo, I., Gratton, R., Ghinassi, F., and Lodi, M.: 2014, in *Society of Photo-Optical Instrumentation Engineers (SPIE) Conference Series*, Vol. 9147 of *Society of Photo-Optical Instrumentation Engineers (SPIE) Conference Series*, p. 1
- Piskunov, N. E., Kupka, F., Ryabchikova, T. A., Weiss, W. W., and Jeffery, C. S.: 1995, *A&A Supp.* **112**, 525
- Quirrenbach, A., Amado, P. J., Caballero, J. A., Mundt, R., Reiners, A., Ribas, I., Seifert, W., Abril, M., Aceituno, J., Alonso-Floriano, F. J., Ammler-von Eiff, M., Antona Jiménez, R., Anwand-Heerwart, H., Azzaro, M., Bauer, F., Barrado, D., Becerril, S., Béjar, V. J. S., Benítez, D., Berdiñas, Z. M., Cárdenas, M. C., Casal, E., Claret, A., Colomé, J., Cortés-Contreras, M., Czesla, S., Doellinger, M., Dreizler, S., Feiz, C., Fernández, M., Galadí, D., Gálvez-Ortiz, M. C., García-Piquer, A., García-Vargas, M. L., Garrido, R., Gesa, L., Gómez Galera, V., González Álvarez, E., González Hernández, J. I., Grözing, U., Guàrdia, J., Guenther, E. W., de Guindos, E.,

- Gutiérrez-Soto, J., Hagen, H.-J., Hatzes, A. P., Hauschildt, P. H., Helmiling, J., Henning, T., Hermann, D., Hernández Castaño, L., Herrero, E., Hidalgo, D., Holgado, G., Huber, A., Huber, K. F., Jeffers, S., Joergens, V., de Juan, E., Kehr, M., Klein, R., Kürster, M., Lamert, A., Lalitha, S., Laun, W., Lemke, U., Lenzen, R., López del Fresno, M., López Martí, B., López-Santiago, J., Mall, U., Mandel, H., Martín, E. L., Martín-Ruiz, S., Martínez-Rodríguez, H., Marvin, C. J., Mathar, R. J., Mirabet, E., Montes, D., Morales Muñoz, R., Moya, A., Naranjo, V., Ofir, A., Oreiro, R., Pallé, E., Panduro, J., Passegger, V.-M., Pérez-Calpena, A., Pérez Medialdea, D., Perger, M., Pluto, M., Ramón, A., Rebolo, R., Redondo, P., Reffert, S., Reinhardt, S., Rhode, P., Rix, H.-W., Rodler, F., Rodríguez, E., Rodríguez-López, C., Rodríguez-Pérez, E., Rohloff, R.-R., Rosich, A., Sánchez-Blanco, E., Sánchez Carrasco, M. A., Sanz-Forcada, J., Sarmiento, L. F., Schäfer, S., Schiller, J., Schmidt, C., Schmitt, J. H. M. M., Solano, E., Stahl, O., Storz, C., Stürmer, J., Suárez, J. C., Ulbrich, R. G., Veredas, G., Wagner, K., Winkler, J., Zapatero Osorio, M. R., Zechmeister, M., Abellán de Paco, F. J., Anglada-Escudé, G., del Burgo, C., Klutsch, A., Lizon, J. L., López-Morales, M., Morales, J. C., Perryman, M. A. C., Tulloch, S. M., and Xu, W.: 2014, in *Society of Photo-Optical Instrumentation Engineers (SPIE) Conference Series*, Vol. 9147 of *Society of Photo-Optical Instrumentation Engineers (SPIE) Conference Series*, p. 1
- Ramírez, I., Allende Prieto, C., and Lambert, D. L.: 2013, *ApJ* **764**, 78
- Ramírez, I., Fish, J. R., Lambert, D. L., and Allende Prieto, C.: 2012, *ApJ* **756**, 46
- Ramírez, I. and Meléndez, J.: 2005a, *ApJ* **626**, 446
- Ramírez, I. and Meléndez, J.: 2005b, *ApJ* **626**, 465
- Rayner, J., Bond, T., Bonnet, M., Jaffe, D., Muller, G., and Tokunaga, A.: 2012, in *Ground-based and Airborne Instrumentation for Astronomy IV*, Vol. 8446 of *Proceedings of the SPIE*, p. 84462C
- Rayner, J., Tokunaga, A., Jaffe, D., Bonnet, M., Ching, G., Connelley, M., Kokubun, D., Lockhart, C., and Warmbier, E.: 2016, in *Society of Photo-Optical Instrumentation Engineers (SPIE) Conference Series*, Vol. 9908 of *Proceedings of the SPIE*, p. 990884
- Recio-Blanco, A., Bijaoui, A., and de Laverny, P.: 2006, *MNRAS* **370**, 141
- Santos, N. C., Adibekyan, V., Figueira, P., Andreasen, D. T., Barros, S. C. C., Delgado-Mena, E., Demangeon, O., Faria, J. P., Oshagh, M., Sousa, S. G., Viana, P. T. P., and Ferreira, A. C. S.: 2017, *ArXiv e-prints*
- Santos, N. C., Israelian, G., and Mayor, M.: 2004, *A&A* **415**, 1153
- Santos, N. C., Sousa, S. G., Mortier, A., Neves, V., Adibekyan, V., Tsantaki, M., Delgado Mena, E., Bonfils, X., Israelian, G., Mayor, M., and Udry, S.: 2013, *A&A* **556**, A150
- Sato, B., Izumiura, H., Toyota, E., Kambe, E., Ikoma, M., Omiya, M., Masuda, S., Takeda, Y., Murata, D., Itoh, Y., Ando, H., Yoshida, M., Kokubo, E., and Ida, S.: 2008, *PASJ* **60**, 539
- Sato, B., Omiya, M., Harakawa, H., Izumiura, H., Kambe, E., Takeda, Y., Yoshida, M., Itoh, Y., Ando, H., Kokubo, E., and Ida, S.: 2012, *PASJ* **64**
- Sato, B., Omiya, M., Harakawa, H., Liu, Y.-J., Izumiura, H., Kambe, E., Takeda, Y., Yoshida, M., Itoh, Y., Ando, H., Kokubo, E., and Ida, S.: 2013, *PASJ* **65**
- Smiljanic, R., Korn, A. J., Bergemann, M., Frasca, A., Magrini, L., Masseron, T., Pancino, E., Ruchti, G., San Roman, I., Sbordone, L., Sousa, S. G., Tabernero, H., Tautvaišienė, G., Valentini,

- M., Weber, M., Worley, C. C., Adibekyan, V. Z., Allende Prieto, C., Barisevičius, G., Biazzo, K., Blanco-Cuaresma, S., Bonifacio, P., Bragaglia, A., Caffau, E., Cantat-Gaudin, T., Chorniy, Y., de Laverny, P., Delgado-Mena, E., Donati, P., Duffau, S., Franciosini, E., Friel, E., Geisler, D., González Hernández, J. I., Gruyters, P., Guiglion, G., Hansen, C. J., Heiter, U., Hill, V., Jacobson, H. R., Jofre, P., Jönsson, H., Lanzafame, A. C., Lardo, C., Ludwig, H.-G., Maiorca, E., Mikolaitis, Š., Montes, D., Morel, T., Mucciarelli, A., Muñoz, C., Nordlander, T., Pasquini, L., Puertas, E., Recio-Blanco, A., Ryde, N., Sacco, G., Santos, N. C., Serenelli, A. M., Sordo, R., Soubiran, C., Spina, L., Steffen, M., Vallenari, A., Van Eck, S., Villanova, S., Gilmore, G., Randich, S., Asplund, M., Binney, J., Drew, J., Feltzing, S., Ferguson, A., Jeffries, R., Micela, G., Negueruela, I., Prusti, T., Rix, H.-W., Alfaro, E., Babusiaux, C., Bensby, T., Blomme, R., Flaccomio, E., François, P., Irwin, M., Koposov, S., Walton, N., Bayo, A., Carraro, G., Costado, M. T., Damiani, F., Edvardsson, B., Hourihane, A., Jackson, R., Lewis, J., Lind, K., Marconi, G., Martayan, C., Monaco, L., Morbidelli, L., Prisinzano, L., and Zaggia, S.: 2014, *A&A* **570**, A122
- Snedden, C. A.: 1973, *Ph.D. thesis*, THE UNIVERSITY OF TEXAS AT AUSTIN.
- Soubiran, C., Le Campion, J.-F., Brouillet, N., and Chemin, L.: 2016, *A&A* **591**, A118
- Sousa, S. G., Santos, N. C., Adibekyan, V., Delgado-Mena, E., and Israelian, G.: 2015, *A&A* **577**, A67
- Sousa, S. G., Santos, N. C., Israelian, G., Mayor, M., and Monteiro, M. J. P. F. G.: 2007, *A&A* **469**, 783
- Sousa, S. G., Santos, N. C., Israelian, G., Mayor, M., and Udry, S.: 2011, *A&A* **533**, A141
- Sousa, S. G., Santos, N. C., Mayor, M., Udry, S., Casagrande, L., Israelian, G., Pepe, F., Queloz, D., and Monteiro, M. J. P. F. G.: 2008, *A&A* **487**, 373
- Takeda, Y., Sato, B., and Murata, D.: 2008, *PASJ* **60**, 781
- Torres, G., Andersen, J., and Giménez, A.: 2010, *Astronomy and Astrophysics Reviews* **18**, 67
- Torres, G., Fischer, D. A., Sozzetti, A., Buchhave, L. A., Winn, J. N., Holman, M. J., and Carter, J. A.: 2012, *ApJ* **757**, 161
- Torres, G., Winn, J. N., and Holman, M. J.: 2008, *ApJ* **677**, 1324
- Tsantaki, M., Andreasen, D. T., Teixeira, G. D. C., Sousa, S. G., Santos, N. C., Delgado-Mena, E., and Bruzual, G.: 2017, *MNRAS* **555**, A150
- Tsantaki, M., Sousa, S. G., Adibekyan, V. Z., Santos, N. C., Mortier, A., and Israelian, G.: 2013, *A&A* **555**, A150
- Tsantaki, M., Sousa, S. G., Santos, N. C., Montalto, M., Delgado-Mena, E., Mortier, A., Adibekyan, V., and Israelian, G.: 2014, *A&A* **570**, A80
- Valenti, J. A. and Fischer, D. A.: 2005, *ApJS* **159**, 141
- Valenti, J. A. and Piskunov, N.: 1996, *A&A Supp.* **118**, 595
- Zieliński, P., Niedzielski, A., Wolszczan, A., Adamów, M., and Nowak, G.: 2012, *A&A* **547**, A91